IEEE Access
Multidisciplinary | Rapid Review | Open Access Journal

Received June 28, 2019, accepted July 6, 2019, date of publication July 9, 2019, date of current version July 26, 2019.

Digital Object Identifier 10.1109/ACCESS.2019.2927635

Novel Series Arc Fault Detector Using High-Frequency Coupling Analysis and Multi-Indicator Algorithm

GUANGHAI BAO, RUN JIANG, AND XIAOQING GAO
College of Electrical Engineering, Fuzhou University, Fuzhou 350108, China
Fujian Key Laboratory of New Energy Generation and Power Conversion, Fuzhou 350108, China
Corresponding author: Guanghai Bao (19428733@qq.com)

ABSTRACT In the field of arc fault detection, it is universally acknowledged that it is very hard to judge whether there is an arc fault through signals of the main line when a masking load (such as air compressors, lamps with dimmers, and so on) is in parallel with a resistive load, which always tends to be a fire hazard. Meanwhile, it is annoying that the normal currents of some appliances are very similar to the arcing ones. In this paper, we have found the principles of a novel detection method called high-frequency coupling, putting the neutral line (N) and the live line (L) through the current transformer (CT), which results in asymmetrical distribution of magnetic flux in the core and the only high-frequency components left in the secondary output of the CT. So it is possible for series arc fault detectors to be free from the masking loads and distinguish between the arcing and the nonarcing clearly. Thanks to this convenient method, an arc fault detector based on the microcontroller unit (MCU) has been proposed to detect arc faults effectively by means of simple multi-indicators. The experimental results show the accuracy of arc fault recognition, in all the masking tests, can reach a high level and the detector can detect an arc fault within a short time.

INDEX TERMS Series arc fault, high-frequency coupling, asymmetrical distribution, magnetic flux, multi-indicators, detector, MCU, masking tests.

I. INTRODUCTION

According to the latest report on topical fires from U.S. Fires Administration (Dec. 2018), about 24000 residential building electrical fires occurred each year from 2014 to 2016, which leads to injury, claims lives and causes large losses of property. Presently, circuit breakers in residential buildings still lack a good-performance part on arc fault detection. So, fires mainly caused by arc faults still exist, although research on arc faults lasts for many years. Arc fault circuit interrupters (AFCIs) are regarded as one of the most promising devices, because they can solve problems of electrical fire hazards to much extent. Wherein, the arc fault detection method is of significance in the production of AFCIs, which will matter whether the devices can be commercialized with low cost. More importantly, it also matters whether missed judgment and misjudgment will occur. The traditional way to detect arc faults focuses on current signals from the main line. However, it is very difficult to identify arc faults unless complex signal processing is used, because the arcing current waveform varies with the load type. What is worse, the arcing current can hardly be found if there is a arc fault in a low-power branch circuit, and some appliance currents in the normal condition are very similar to the arcing ones, such as fluorescent lamps, lamps with a dimmer and so on.

Recently, machine learning algorithms have been widely studied in the field of arc fault detection for its autonomous learning, such as the support vector machine, the neutral network, etc [1]–[3]. [4] has proposed a new neutral network called the SRFCNN method which contains a pretreatment layer, a sparse representation layer and a decision layer. After it is trained many times, the general classification precision of some loads can reach 94.3%. [5] identifies series arc faults based on principal component analysis and support vector machine (PCA-SVM). Experimental loads are separated according to the load type firstly, and then the accuracy of detection can reach a high level after the principal components obtained by PCA train Back Propagation Neutral Network (BPNN). [6] uses time-frequency and time-domain extracted features with hidden Markov models (HMMs), which are suitable for detection of nonstationary signals of arc faults. In addition, cluster analysis has been applied in this

The associate editor coordinating the review of this manuscript and approving it for publication was Abdullah Iliyasu.

field, too [7]. However, it can be seen from the above articles that these algorithms can only be processed by computers for complexity of training, which will make dwellers unwilling to purchase such a device for high cost and big sizes. Meanwhile, there are not enough load types in their experiments, which probably results in low feasibility in practice.

Generally speaking, the methods on frequency domain analysis of arcing current are more practical than the above ones, because they are easier to be achieved. However, the speed of identifying arc faults will be influenced by a high sampling rate to avoid missing some frequency domain information, such as Fourier Transformation [8], [9], wavelet transformation [10]–[12], etc [13]. In order to solve this problem, a high-performance MCU is required. To achieve the detection of arc faults easily, some unique physical characteristics of arc faults are also introduced to detect arc faults, such as sound and ultra-violet [14], which is limited to the locations where arc faults occur. The detection on arcing electromagnetic radiation is an interesting topic which is investigated by [15]–[17]. In addition to the aforementioned methods, the detection methods on the time domain characteristics of arcing current are also a hot topic and they are most likely to be achieved if the characteristics can be extracted in a simple way. [18] uses the arcing current derivative to identify arc faults, but this method fails in switched mode loads. [19] identifies arc faults though analysis of arcing current and arcing voltage. In [20], a Kalman filter is used to get first arcing fault factors. Then, the factors are confirmed again by a Fuzzy logic processor whether they indicate there is an arc fault. There are many limitations if the zero crossing time (shoulder) is used to detect arc faults, because normal current waveforms of lamps with dimmers have the similar shoulders and shoulders of some loads are hard to be found. So, an extra indicator must be added [21]. Among patents published in American, many methods extract high-frequency components of current signals to recognize complicated arc faults. PAT. NO. 10228407 describes a super regenerative high-frequency receiver applied in AFCIs. PAT. NO. 9337643 uses a filter unit to get a frequency higher than a cut-off frequency and analyses the remaining signals in the time domain. PAT. NO. 8421473 provides a voltage zero crossing detector and a high- frequency sensor for high-frequency current signals. PAT. NO. 5815352 provides a multiple stages of high pass filter to count the number of pulses.

The traditional literatures and patents (such as PAT. NO. 9696363, PAT. NO. 9 664723, PAT. NO. 9640968) always focus on signals of one line. Few methods make use of signals of two lines (the neutral line and the live line). G. Bao et al. proposed this novel detection method and did experimental research to verify feasibility of it, but they did not explain principles of this new method in detail and develop an arc fault detection device [22]. In this paper, we report principles of this method called high-frequency coupling, putting the neutral line and the live line in asymmetrical locations of CT, which results in asymmetrical distribution of magnetic flux in the core. Unlike traditional methods, the method can detect the high-frequency components and filter the low-frequency ones easily without any complex circuit and signal processing, which can solve the problem of missed judgment in the low-power branch fault. What is more, we have proposed a detector based on high-frequency coupling and a multi-indicator algorithm, and this detector performs very well in all the masking tests in accordance with UL1699 [23], which have not been attempted in many literatures at present.

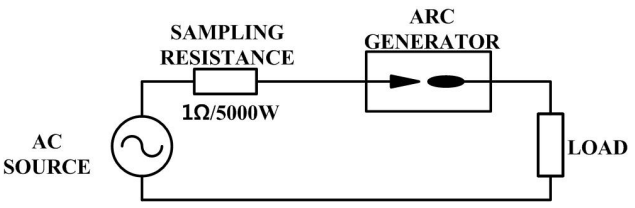

FIGURE 1. The experimental platform.

II. ANALYSIS OF ARC FAULT CURRENT

Fig. 1 shows the experimental platform to analyze characteristics of arc fault current, which contains an ac source, a sampling resistance which is used to acquire signals of currents, a load and an arc generator which is made according to UL1699. Arcing current waveforms have some common characteristics, such as the zero crossing time (shoulders), the arcing current values lower than the common ones and a wide frequency range. [24] shows the arc resistance has the characteristic of oscillation. So there are abundant oscillating components of high frequency in currents of arbitrary loads (resistive loads, inductive loads and non-linear loads) when arc faults occur, which are shown in Fig. 2. The detector will fail to identify arc faults in some loads, if the shoulders or the rising rate after the shoulders is used as a feature, because normal currents of some appliances have the similar characteristics.

To achieve detection, the high-frequency oscillating components, which have a wide frequency range, are extracted as features. Therefore, frequency domain analysis of arcing currents is critical for detectors to decide how to set the sampling frequency. Frequency domain information is obtained by means of Fast Fourier Transformation (FFT). As shown in Fig. 3, the frequency of arcing currents also distributes in the area below several hundred kilohertz, although its frequency can reach MHz [25]. In this paper, we focus on the information of the current below 400 kHz.

III. PROPOSED SOLUTIONS

A. INTRODUCTION OF DETECTOR HARDWARE

Fig. 4 shows the schematic diagram of the hardware structure, which contains signal acquisition (high-frequency coupling), signal processing (signal conditioning circuit and MCU) and fault warning (indicator lamp).

- **Signal acquisition**: the current transformer, with a maximum bandwidth of 10MHz, has a stable magnetic

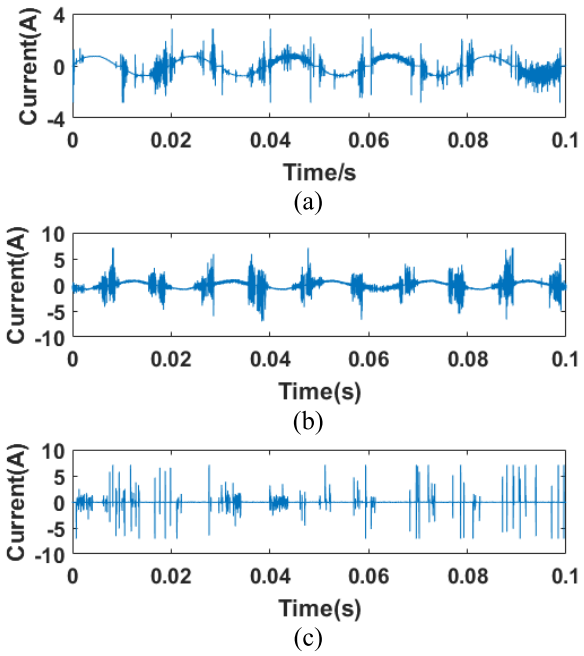

FIGURE 2. The arcing current waveforms of some loads. (a) the incandescent lamp. (b) the hand drill. (c) the fluorescent lamp.

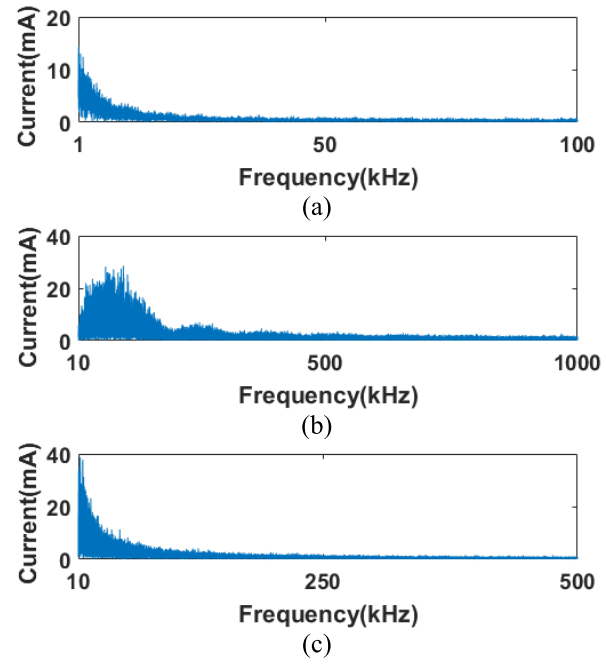

FIGURE 3. Frequency domain analysis of some loads. (a) the incandescent lamp. (b) the hand drill. (c) the fluorescent lamp.

permeability below 10MHz and is selected for acquisition of high-frequency signals. Fig. 5 shows the novel arc fault detection method, which is named high-frequency coupling, to put the neutral line and the live line in asymmetrical locations, which results in asymmetrical distribution of flux in the core.

The ideal relationship between the current and its corresponding magnetic flux can be expressed approximately as

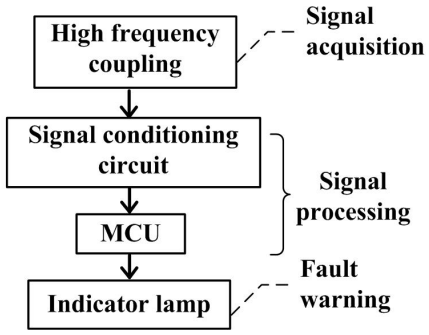

FIGURE 4. The schematic diagram of the hardware structure.

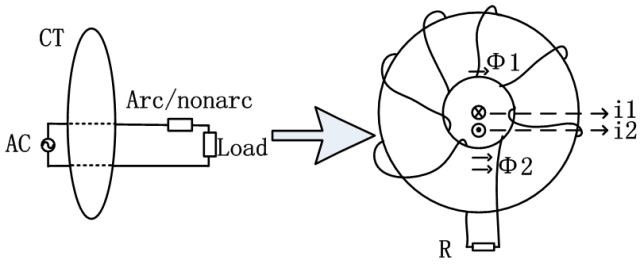

FIGURE 5. The high-frequency coupling method.

follows:

$$\phi_1 = k_+ i_1 \quad \phi_2 = k_- i_2 \tag{1}$$

where k_+ and k_- are linear factors.

Suppose i_1 to be the sine function. Then, the secondary current can be written as follows:

$$\begin{aligned} i_c &= \frac{N}{R} \cdot \frac{d(\phi_1 + \phi_2)}{dt} = \frac{N}{R} \cdot \frac{d(k_+ i_1 + k_- i_2)}{dt} \\ &= \frac{N \cdot (k_+ - k_-)}{R} \cdot \frac{di_1}{dt} = \frac{N \cdot \chi}{R} \cdot m \cdot \omega \cdot i_1 \end{aligned} \tag{2}$$

where N is the coil turns, $\chi (= k_+ - k_-)$ is a so small value that the secondary current is almost zero if i_1 is low frequency current, ω is the angular frequency of the fundamental wave and m is the harmonic order.

For simplifying analysis, the arcing current can be Fourier expanded through odd prolongation due to limit of the observation window when arc faults occur.

$$\begin{aligned} i_{arc}(t) &= \frac{a_0}{2} + \sum_{m=1}^{\infty} [a_m \cos(m\omega t) + b_m \sin(m\omega t)] \\ a_m &= \frac{1}{\pi} \int_{-\pi}^{\pi} i_{arc}(t) \cos(m\omega t) d(\omega t) = 0 \\ b_m &= \frac{1}{\pi} \int_{-\pi}^{\pi} i_{arc}(t) \sin(m\omega t) d(\omega t), \quad m = 0, 1, \ldots, \infty. \end{aligned} \tag{3}$$

Then, the arcing current is

$$i_{arc}(t) = \sum_{m=1}^{\infty} b_m \sin(m\omega t) \tag{4}$$

According to (2), i_c can be expressed as follows:

$$i_c = \frac{N}{R} \cdot \frac{d\{\sum_{m=1}^{\infty} [\chi_m \cdot b_m \cdot \sin(m\omega t)]\}}{dt} \tag{5}$$

Suppose that $\overline{\chi}$ is not related to m and can replace χ_m:

$$\begin{aligned} i_c &= \frac{N}{R} \cdot \chi \cdot \frac{di_{arc}}{dt} \\ u_c &= \chi_{arc} \cdot \frac{di_{arc}}{dt} \\ \frac{di_{arc}}{dt} &\underset{\rightarrow}{discretization} \frac{i_{arc}(kT+T)-i_{arc}(kT)}{T}(k=0,1,2\ldots) \end{aligned} \tag{6}$$

where u_c is the secondary voltage, T is the sampling period (100ns) and χ_{arc} is a very small value.

It can be seen from the above analysis that the high-frequency coupling signal is related to the arcing current and this method can detect the high-frequency components and filter the low frequency ones easily without any complex circuit and signal processing. When an arc fault occurs, the output signals of the secondary circuit show a series of pulses. The parameter χ_{arc} depends on the transformer used and the position of the cables in the transformer. Therefore, it can be determined only after a certain transformer is selected and the locations of the two cables are fastened. If the transformer used performs not well in high frequency, it will weaken the coupling signals of arcing current. Meanwhile, if the two cables are put in approximately symmetric locations, it will weaken the coupling signals, too. Since the cables can not be put in absolutely symmetric locations, the parameter is always bigger than 0. In order to overcome them, we selected the transformer, which performs well in high frequency, to obtain distinct coupling signals of arc faults and the hole of the transformer used can just accommodates two cables. χ_{arc} is approximately $4 \times 10^{-9} V \cdot s/A$ through experiments of many loads. Fig. 6 shows actual and calculated waveforms of high-frequency coupling to verify correctness of the principle (according to the formula (6), the calculated waveform is obtained based on the actual arcing current).

- **Signal processing**: the signal conditioning circuit includes a low-pass filter and a voltage-lift part with function of amplification in Fig. 7. The transfer function of the low-pass filter can be written as:

$$\begin{aligned} \frac{U_1(s)}{U_c(s)} &= \frac{1}{-[C_1C_2R_1R_2S^2 + C_2(R_2 + R_1 + \frac{R_1R_2}{R_3})S + \frac{R_1}{R_3}]} \\ &\approx -\frac{1}{(\frac{S}{2\pi \cdot 400000})^2 + \sqrt{2} \cdot \frac{S}{2\pi \cdot 400000} + 1} \end{aligned} \tag{7}$$

The formula (7) shows the filter has a cut-off frequency of 400kHz. The voltage-lift part is used to move up the whole input signals in order to guarantee the MCU can get positive voltage and the amplifying coefficient (= 10) can identify arc faults more easily. The expression between U2 and U1 can be

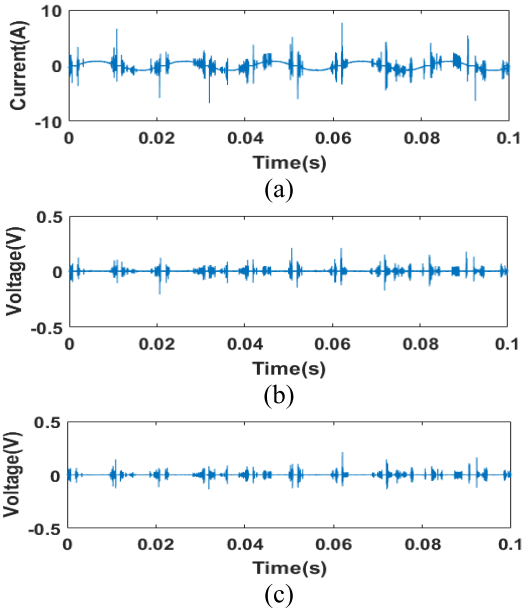

FIGURE 6. Comparison between the actual coupling waveform and the calculated coupling waveform. (a) the arcing current waveform. (b) the actual waveform of high-frequency coupling. (c) the calculated waveform of high-frequency coupling.

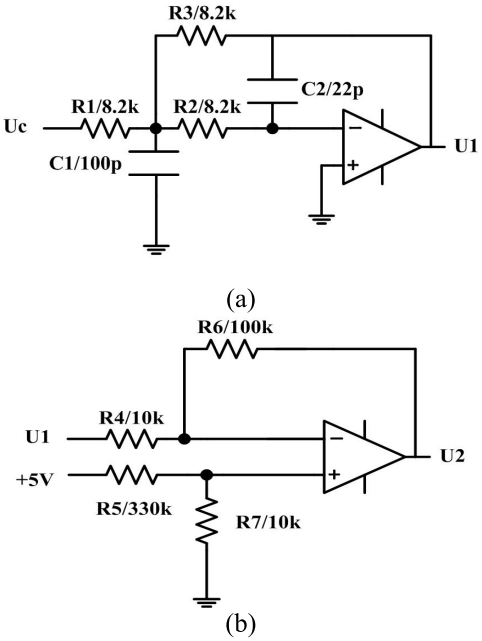

FIGURE 7. The signal conditioning circuit. (a) the low-pass filter. (b) the voltage-lift part with function of an amplification.

written as:

$$\begin{aligned} U_2(t) &= -\frac{R_6}{R_4} \cdot U_1(t) + 5 \cdot \frac{R_7(R_4 + R_6)}{R_4(R_5 + R_7)} \\ &\approx -10U_1 + 1.6 \end{aligned} \tag{8}$$

A 32-bit MCU named PIC32MZ1024EFH064 is used to acquire voltage signals with a sampling rate of 1MHz and the working speed of the CPU is 200 MHz.

- **Fault warning**: the lamp will be lit if arc faults are detected.

B. INTRODUCTION OF DETECTOR SOFTWARE

1) INDICATORS

- **PULSE1:** The number of groups, where the maximum values range from A_1 to A_2, after the finite difference results of the k samples $(S_1 \cdots S_k)$, in the fixed observation window (T), are divided into y groups equally $(W_1 \cdots W_y)$.

$$g(i) = \begin{cases} 1, & A_1 \le \max(W_i) \le A_2 \\ 0, & \max(W_i) < A_1 \\ 0, & \max(W_i) > A_2 \end{cases}$$

$$PULSE1 = \sum_{i=1}^{y} g(i) \tag{9}$$

- **PULSE2**: The number of groups, where the maximum values are bigger than A_2. after the finite difference results of the k samples $(S_1 \cdots S_k)$, in the fixed observation window (T), are divided into y groups equally $(W_1 \cdots W_y)$

$$y(i) = \begin{cases} 1, & \max(W_i) > A_2 \\ 0, & \max(W_i) \le A_2 \end{cases}$$

$$PULSE2 = \sum_{i=1}^{y} y(i) \tag{10}$$

- **SUM**: The value of PULSE1 plus PULSE2.

$$SUM = PULSE1 + PULSE2 \tag{11}$$

2) DETECTION STRATEGY

The core of PULSE1 and PULSE2 is finite difference, which is very sensitive to high-frequency pulses. In a word, the indicator PULSE1 means the number of groups which contain small pulses. The indicator PULSE2 means the number of groups which contain big pulses. Since the arcing waveforms have many small pulses and big pulses (see Fig. 8), PULSE1 and PULSE2 can be used to identify whether there is an arc fault or not.

Thanks to the high-frequency coupling method, the coupling signals of most loads are nearly zero when they are under normal operation, and the coupling signals show a series of pulses when they are under arc fault operation, which is shown in Fig. 8 (a)(b). However, in Fig. 8(c), when the lamps with a dimmer are in normal operation, the signals also have pulses. What is more, the arcing waveform is a little similar to the nonarcing one. The critical problem is how to solve similarity between the arcing coupling signals and the nonarcing ones in the lamps with a dimmer. Fortunately, the arcing coupling signals have many groups that contain small pulses, but the nonarcing ones do not have this characteristic. Because the pulses of normal operation are

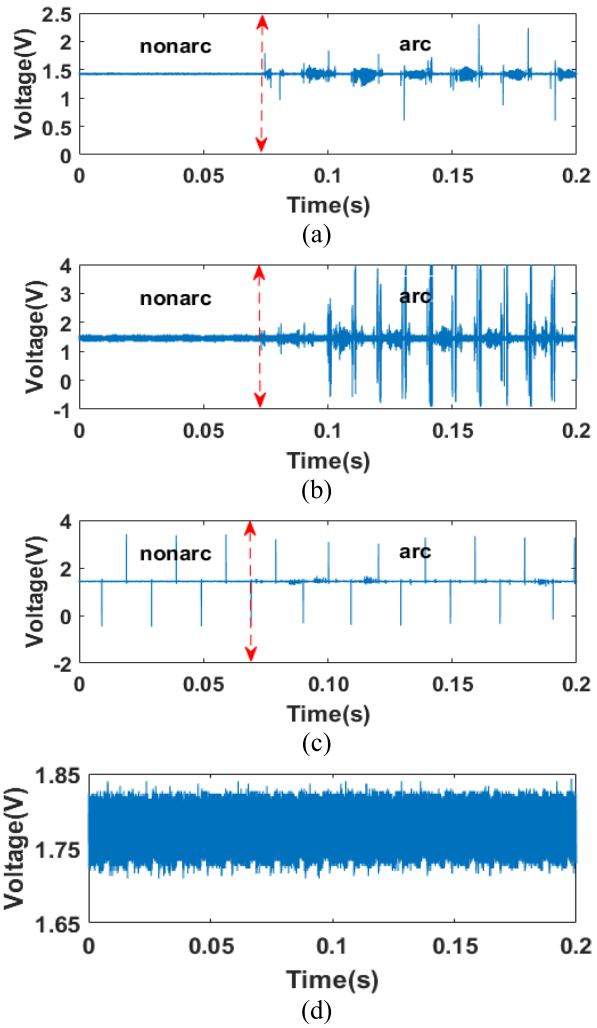

FIGURE 8. The high-frequency coupling signals and noise signals. (a) the kettle. (b) the vacuum cleaner. (c) the lamps with a dimmer. (d) radio noise.

few and dense and the arcing pulses are many and disperse, we divide the finite difference results of the k samples into y groups. When arc faults occur, many of y groups show pulses. When arc faults do not occur, few of y groups show pulses. The time width of the nonarcing pulses we measured in the dimmer load is around 10us. Therefore, the time width of each group we set is 20us to cover the nonarcing pulses. The sampling rate is 1MHz and the calculating cycle is 100ms. So, k is 100000 and y is 5000. The reason why we set the sampling rate to be 1MHz is that we focus on the current information below 400KHz, and the reason why we set the calculating cycle to be 100ms is that the longer the calculating cycle is, the more information processed signals will contain, which is helpful for the detector to judge whether there is an arc fault. We found finite difference results of small pulses of the lamps with a dimmer are smaller than 10 and bigger than 3 under arcing operation. This is the reason why A_1 is 3 and A_2 is 10 in the formula of PULSE1 and PULSE2. The indicator SUM is used to be immune to high-frequency noise

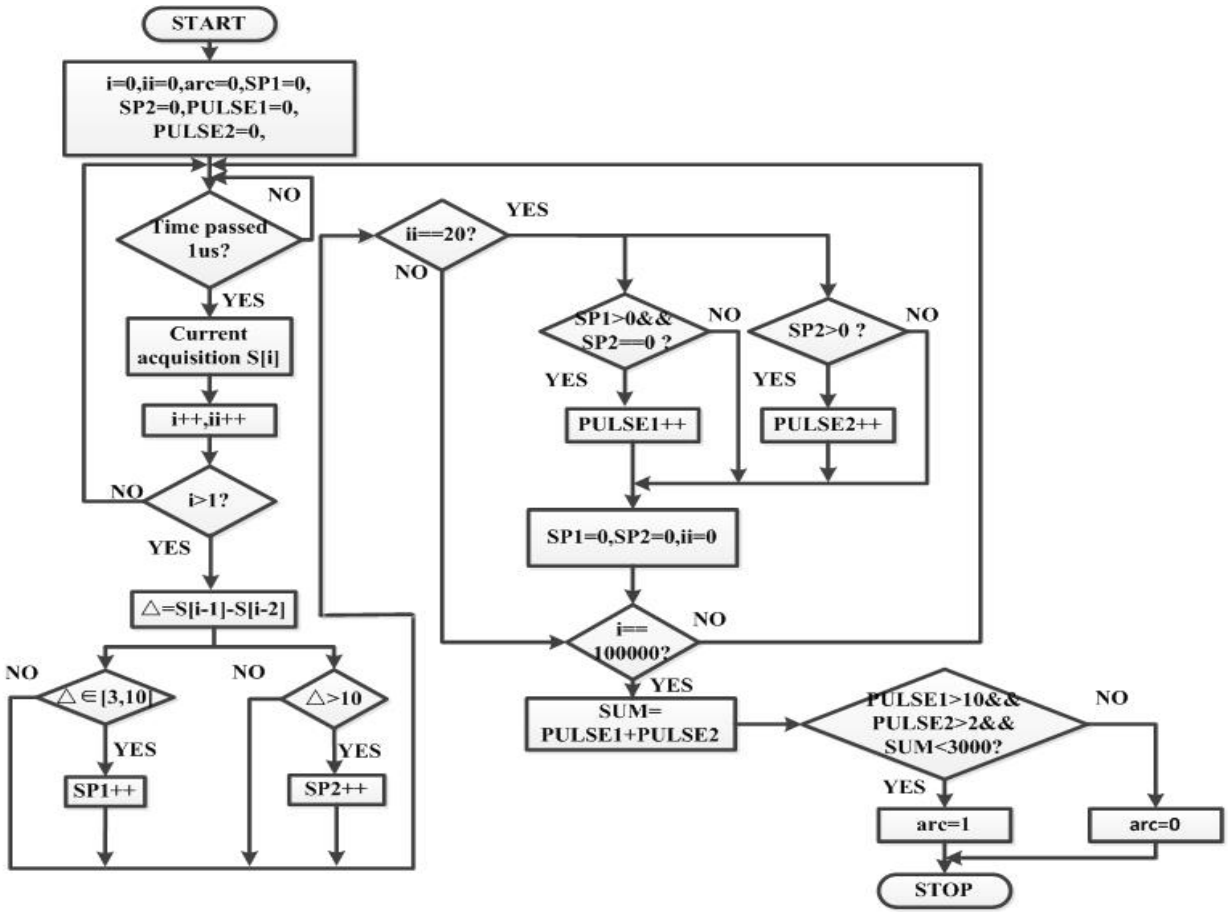

FIGURE 9. Flowchart of the strategy each 100ms.

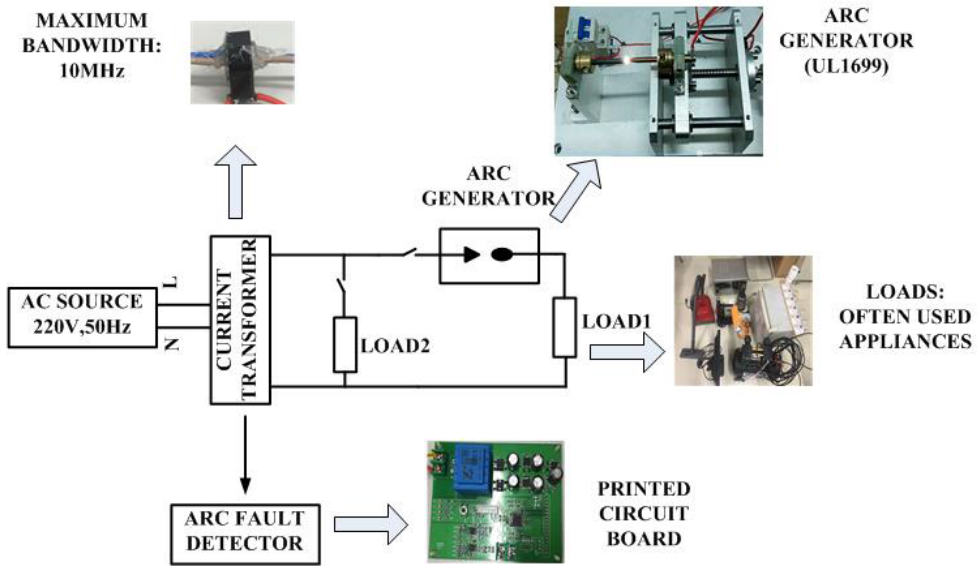

FIGURE 10. Schematic of experiments.

signals from the two way radio. As it can be seen from the noise waveform as shown in Fig. 8 (d), the noise pulses are much more than the arcing ones, because they contain too many big and small pulses.

The thresholds for these indicators are obtained from experiments. The representative loads we selected are a resistance load, a vacuum cleaner (inductive load), lamps with a dimmer (nonlinear load). According to the TABLE 1,

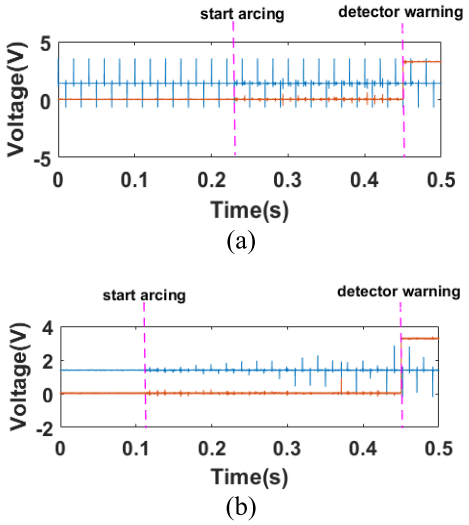

FIGURE 11. Judgment time of each load. (a) the lamps with a dimmer. (b) the 3A resistance.

TABLE 1. Results of three-time experiments.

LOAD	PULSE1	PULSE2	SUM
3A resistance (normal)	PULSE1≤2	PULSE2=0	SUM≤2
Vacuum cleaner (normal)	PULSE1≤2	PULSE2=0	SUM≤8
Lamps with a dimmer (normal)	PULSE1≤7	PULSE2≤10	SUM≤17
3A resistance (arcing)	PULSE1≥13	PULSE2≥3	16≤SUM≤3000
Vacuum cleaner (arcing)	PULSE1≥500	PULSE2≥40	540≤SUM≤3000
Lamps with a dimmer (arcing)	PULSE1≥20	PULSE2≥8	34≤SUM≤3000
Radio noise (near location)	PULSE1≥2000	PULSE2≥2000	SUM ≥4000
Radio noise (far location)	PULSE1⩾0	PULSE2=0	SUM ⩾0

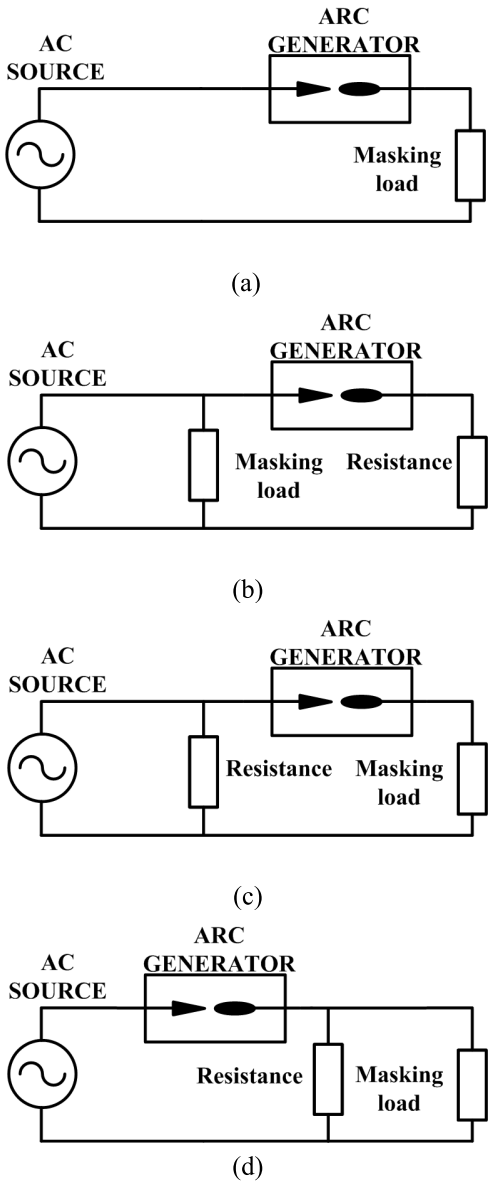

FIGURE 12. Masking experiments. (a) configuration A. (b) configuration B. (c) configuration C. (d) configuration D.

the maximum PULSE1 of nonarcing situation is 7 and the minimum PULSE1 of arcing situation is 13. So, the threshold of PULSE1 can be set as 10. However, PULSE1 of radio noise may be bigger than 10. Therefore, the another indicator, PULSE2, is necessary. The maximum PULSE2 of nonarcing situation is 10 and the minimum PULSE2 of arcing situation is 8. It is because the arcing waveform is a little similar to the nonarcing one in the dimmer load, which results in difficulty to distinguish between the nonarcing PULSE2 and the arcing PULSE2. Although the PULSE2 of the lamps with a dimmer is less than 10 in normal operation, the threshold of PULSE2 can be set as 2, because the PULSE1 of the lamps with a dimmer is less than 7 in normal operation and its corresponding threshold is 10. The threshold of SUM can be set as 3000, because SUM of the radio noise is more than 4000 in a near location and SUM of arc faults in arbitrary load is less than 3000.

The flowchart can be seen in Fig. 9. Briefly speaking, the cycle of calculation is set as 100ms (T) and the sampling rate is 1MHz. A_1, A_2 and y have been set as 3, 10 and 5000, respectively, and the thresholds of PULSE1, PULSE2 and SUM have been set as 10, 2 and 3000, respectively. The detector obtains $k(100000)$ samples each 100ms. Then, those indicators can be obtained after the k samples are acquired in the form of digital signals, because it is not necessary to invert the obtained digital quantity to analog quantity again, which can decrease the time of calculation. With the obtained indicators at the end of each cycle, the detector is able to judge whether

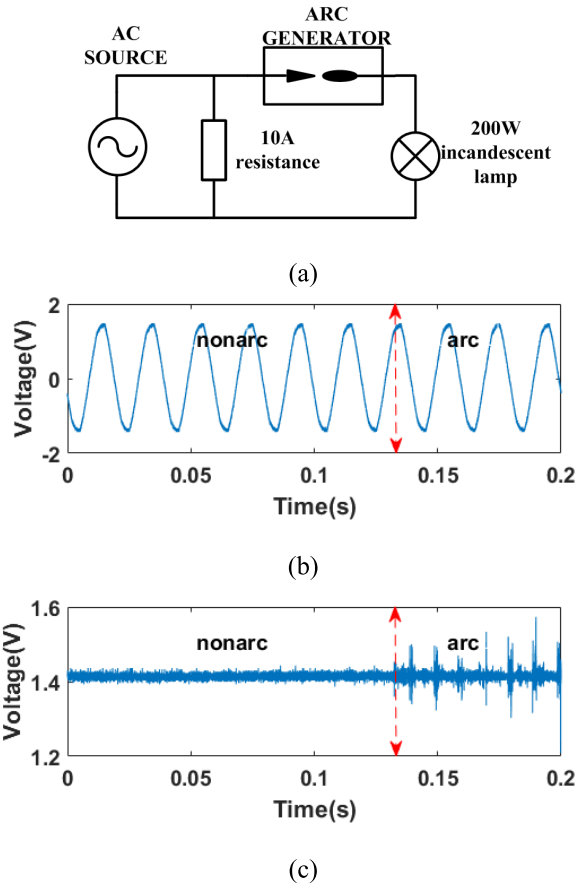

FIGURE 13. A 200W fault branch in parallel with a 10A resistance. (a) the schematic. (b) the main circuit signal. (c) the output signal of the conditioning circuit.

the samples are arcing ones. In consideration of misjudgment caused by starting process of loads, we require that the detector can identify there is an arc fault only if the result of arc=1 appears at least 3 times (300ms) in 5 times of calculations (500ms). Therefore, the time of judgment is at least bigger than 200ms.

IV. EXPERIMENTAL INTRODUCTION AND RESULTS

Fig. 10 shows the schematic of experiments. The detection is carried out by the detector which is made through the printed circuit board. The warning part of the detector is a red light. How we calculate the judgment time of arc faults can be found in Fig. 11, where the blue line is the coupling signals, the red line is the light signals, and the purple line is used to measure the judgment time of arc faults. When there is no arc fault, the light is dark (low-level voltage). When there occur arc faults, the light will turn red (high-level voltage).

The loads include a compressor, a vacuum cleaner, three 200W incandescent lamps with a dimmer, two 40W fluorescent lamps, three 85W energy saving lamps, a refrigerator, a microwave oven, a hand drill, a rotary hammer, a kettle,

TABLE 2. Results of detection in various loads.

Load	Test times	Unwanted trips or failure to trip	Maximum detecting time
Resistance, 3A	20	0	450ms
Resistance, 5A	20	0	640ms
Resistance, 13A	20	0	430ms
Resistance, 20A	20	0	310ms
Incan. lamp, 200W	20	0	510ms
Incan. lamp, 400W	20	0	380ms
Refrigerator	20	0	320ms
Microwave oven	20	0	280ms
Electric hand drill	20	0	370ms
Rotary hammer	20	0	470ms
Kettle	20	0	350ms
iPhone 6s	20	0	300ms
Monitor	20	0	480ms
Configuration A:			
Vacuum cleaner	20	0	380ms
Energy saving lamp, 255W	20	0	300ms
600W lamp, dimmer, max	20	0	270ms
600W lamp, dimmer, middle	20	0	300ms
Fluor. lamp, 80W + resistance, 5A	20	0	310ms
Compressor	20	0	410ms
Desktop	20	0	340ms
Configuration B:			
Vacuum cleaner	20	0	710ms
Energy saving lamp, 255W	20	0	490ms
600W lamp, dimmer, max	20	0	320ms
600W lamp, dimmer,middle	20	0	300ms
Fluor. lamp, 80W + resistance, 5A	20	0	450ms
Compressor	20	0	560ms
Desktop	20	0	650ms
Configuration C:			
Vacuum cleaner	20	0	300ms
Energy saving lamp, 255W	20	0	290ms
600W lamp, dimmer, max	20	0	290ms
600W lamp, dimmer,middle	20	0	280ms
Fluor. lamp, 80W + resistance, 5A	20	0	300ms
Compressor	20	0	350ms
Desktop	20	0	500ms

TABLE 2. ***(Continued.)*** **Results of detection in various loads.**

Configuration D:			
Vacuum cleaner	20	0	310ms
Energy saving lamp, 255W	20	0	310ms
600W lamp, dimmer, max	20	0	300ms
600W lamp, dimmer,middle	20	0	300ms
Fluor. lamp, 80W + resistance, 5A	20	0	300ms
Compressor	20	0	740ms
Desktop	20	0	300ms

some resistances, an iphone 6s and three 200W incandescent lamps. According to UL1699, we have tested the masking experiments (configurations A, B, C and D) twenty times under each masking load. The masking loads include the vacuum cleaner, the air compressor, the 600W lamps with a dimmer, the 255W energy saving lamps, the two fluorescent lamps plus an additional 5A resistance and the desktop. As is shown in Fig. 12, configuration A means there is an arc fault in the circuit of the single masking load. Configuration B means there is an arc fault in the resistive branch when the resistive branch is in parallel with the masking load, and configuration C means there is an arc fault in the masking branch when the resistive branch is in parallel with the masking load. Configuration D means there is an arc fault in the main circuit when the resistive branch is in parallel with the masking load. So, the 3A resistive load is selected to be parallel with the masking load in tests of configuration B, C and D. Based on the above tests, many household appliances used commonly have also been tested. The results can be seen in TABLE 2, including unwanted trip tests, failure to trip tests and judgment time of arc faults. In unwanted trips, we tested staring process of each load by on/off, because starting process of a certain load tends to cause unwanted trips [22]. In failure-to-trip tests, we tested whether the detector can identify arc faults in arcing situations. If the detector can identify them and the warning light turns red, we record the judgment time.

Additionally, we tested an experiment specially three times in Fig. 13, a low-power branch fault (a 200 W incandescent lamp) in parallel with a 10A resistance, where misjudgment situations often occur. As it can be seen from Fig. 13 (b) that the traditional way to detect the main circuit signals fails to find out the arcing signals, because the branch fault signal is so small that it plus a 10A sine signal is almost a 10A sine signal. Fortunately, the coupling method can filter the 10A sine signal and retain the fault one. The output signal of the conditioning circuit is shown in Fig. 13 (c). With the detector, the three judgments are 630ms, 540ms and 700ms.

V. CONCLUSION

In this paper, the authors have proposed a novel series arc fault detector based on the high-frequency coupling and multi-indicators. Meanwhile, the principles of the coupling method have been explained. Because of convenience of this coupling method, a portable detector based on the MCU performs very well in all the tests of masking loads and many household appliances, and these tests have not been attempted in many papers at present. More importantly, the detector solves the problem of missed judgment when the small fault signals are covered by the normal currents of high-power loads.

REFERENCES

[1] Z. Yin, L. Wang, Y. Zhang, and Y. Gao, "A novel arc fault detection method integrated random forest, improved multi-scale permutation entropy and wavelet packet transform," in *Electronics*, vol. 8, no. 4, p. 396, Apr. 2019. doi: 10.3390/electronics8040396.

[2] J.-H. Yang, H.-Y. Fang, R.-C. Zhang, and K. Yang, "An arc fault diagnosis algorithm using multiinformation fusion and support vector machines," *Roy. Soc. Open Sci.*, vol. 5, no. 9, Sep. 2018, Art. no. 180160. doi: 10.1098/rsos.180160.

[3] Z. Wang, H. Cao, and J. Liu, "Research on fault arc detection algorithm based on wavelet packet de-noise and EMD decomposition," *Electr. Meas. Instrum.*, vol. 56, no. 6, pp. 117–121, Mar. 2019. doi: 10.19753/j.issn1001-1390.2019.06.020.

[4] Y. Wang, F. Zhang, and S. Zhang, "A new methodology for identifying arc fault by sparse representation and neural network," *IEEE Trans. Instrum. Meas.*, vol. 67, no. 11, pp. 2526–2537, Nov. 2018. doi: 10.1109/TIM.2018.2826878.

[5] J. Jiang, Z. Wen, M. Zhao, Y. Bie, C. Li, M. Tan, and C. Zhang, "Series arc detection and complex load recognition based on principal component analysis and support vector machine," *IEEE Access*, vol. 7, pp. 47221–47229, 2019. doi: 10.1109/ACCESS.2019.2905358.

[6] R. D. Telford, S. Galloway, B. Stephen, and I. Elders, "Diagnosis of series DC Arc faults-A machine learning approach," *IEEE Trans. Ind. Informat.*, vol. 13, no. 4, pp. 1598–1609, Aug. 2017. doi: 10.1109/TII.2016.2633335.

[7] Y. Zhou, W. Wu, and Z. LI, "Low voltage arc fault cluster analysis based on self-organizing map," *Chin. J. Sci. Instrum.*, vol. 31, no. 3, pp. 571–576, Mar. 2010. doi: 10.19650/j.c.nki.cjsi.2010.03.016.

[8] M. K. Khafidli, E. Prasetyono, D. O. Anggriawan, A. Tjahjono, and M. H. R. A. Syafii, "Implementation AC series arc fault recognition using mikrokontroller based on fast Fourier transform," in *Proc. Int. Electron. Symp. Eng. Technol. Appl. (IES-ETA)*, Bali, Indonesia, Jan. 2018, pp. 31–36. doi: 10.1109/ELECSYM.2018.8615529.

[9] H. Cheng, X. Chen, F. Liu, and C. Wang, "Series arc fault detection and implementation based on the short-time Fourier transform," in *Proc. Asia–Pacific Power Energy Eng. Conf.*, Chengdu, China, Mar. 2010, pp. 1–4. doi: 10.1109/APPEEC.2010.5448958.

[10] H.-K. Ji, G. Wang, W.-H. Kim, and G.-S. Kil, "Optimal design of a band pass filter and an algorithm for series arc detection," *Energies*, vol. 11, no. 4, p. 992, Apr. 2018. doi: 10.3390/en11040992.

[11] X. Qin, P. Wang, Y. Liu, L. Guo, G. Sheng, and X. Jiang, "Research on distribution network fault recognition method based on time-frequency characteristics of fault waveforms," *IEEE Access*, vol. 6, pp. 7291–7300, Aug. 2018. doi: 10.1109/ACCESS.2017.2728015.

[12] A. F. Ilman and Dzulkiflih, "Low voltage series arc fault detecting with discrete wavelet transform," in *Proc. Int. Conf. Appl. Eng. (ICAE)*, Batam, Oct. 2018, pp. 1–5. doi: 10.1109/INCAE.2018.8579416.

[13] G. Artale, A. Cataliotti, V. Cosentino, D. Di Cara, S. Nuccio, and G. Tinè, "Arc fault detection method based on CZT low-frequency harmonic current analysis," *IEEE Trans. Instrum. Meas.*, vol. 66, no. 5, pp. 888–896, May 2017. doi: 10.1109/TIM.2016.2627248.

[14] G. Wang, W.-H. Kim, H.-K. Ji, and G.-S. Kil, "Detection and analysis of series arc using non-conventional methods in low-voltage switchboards," *J. Elect. Eng.*, vol. 69, no. 4, pp. 317–322, Aug. 2018. doi: 10.2478/jee-2018-0045.

[15] J. P. Pulkkinen, "Commercial arc fault detection devices in military electromagnetic environment," *IEEE Electromagn. Compat. Mag.*, vol. 7, no. 4, pp. 49–52, 4th Quart., 2018. doi: 10.1109/MEMC.2018.8637290.

[16] R. M. Harris, M. D. Judd, P. J. Moore, and J. Livie, "Radiometric detection and analysis of arcing faults," *IEEE Trans. Dielectr. Electr. Insul.*, vol. 22, no. 3, pp. 1547–1558, Jun. 2015. doi: 10.1109/TDEI.2015.7116350.

[17] Q. Xiong, S. Ji, L. Zhu, L. Zhong, and Y. Liu, "A novel DC arc fault detection method based on electromagnetic radiation signal," *IEEE Trans. Plasma Sci.*, vol. 45, no. 3, pp. 472–478, Mar. 2017. doi: 10.1109/TPS.2017.2653817.

[18] E. Tisserand, J. Lezama, P. Schweitzer, and Y. Berviller, "Series arcing detection by algebraic derivative of the current," *Electr. Power Syst. Res.*, vol. 119, pp: 91-99, Feb. 2015. doi: 10.1016/j.epsr.2014.09.011.

[19] Q. Lu, Z. Ye, Y. Zhang, T. Wang, and Z. Gao, "Analysis of the effects of arc Volt–Ampere characteristics on different loads and detection methods of series arc faults," *Energies*, vol. 12, no. 2, p. 323, Jan. 2019. doi: 10.3390/en12020323.

[20] E. Calderon-Mendoza, P. Schweitzer, and S. Weber, "Kalman filter and a fuzzy logic processor for series arcing fault detection in a home electrical network," *Int. J. Elect. Power Energy Syst.*, vol. 107, pp. 251–263, May 2019. doi: 10.1016/j.ijepes.2018.11.002.

[21] S. H. Ma, J. Q. Bao, Z. Y. Cai, and C. Y. Meng, "A novel arc fault identification method based on information dimension and current zero," *Proc. CSEE*, vol. 36, no. 9, pp. 2572–2579, May 2016. doi: 10.13334/j.0258-8013.pcsee.2016.09.032.

[22] G. Bao, R. Jiang, and D. Liu, "Research on series arc fault detection based on higher-order cumulants," *IEEE Access*, vol. 7, pp. 4586–4597, 2018. doi: 10.1109/ACCESS.2018.2888591.

[23] *Standard for Arc-Fault Circuit Interrupters*, Standard 1699, UL, Northbrook, IL, USA, Apr. 2006.

[24] X. Zhang, A. Bruce, S. Rowland, V. Terzija, and S. Bu, "Modeling the development of low current arcs and arc resistance simulation," *IEEE Trans. Dielectr. Electr. Insul.*, vol. 25, no. 6, pp. 2049–2057, Dec. 2018. doi: 10.1109/TDEI.2018.007100.

[25] C. J. Kim, "Electromagnetic radiation behavior of low-voltage arcing fault," *IEEE Trans. Power Del.*, vol. 24, no. 1, pp. 416–423, Jan. 2009. doi: 10.1109/TPWRD.2008.2002873.

GUANGHAI BAO received the B.S. and Ph.D. degrees in electrical engineering from Fuzhou University, Fujian, China, in 2000 and 2011, respectively, where he is currently an Associate Professor and the Department Head with the College of Electronic Science and Engineering. He was a Postdoctorate with Changshu switching Manufacturing Company Ltd. His research interests mainly include electrical appliances and fault diagnosis.

RUN JIANG received the B.S. degree from Fuzhou University, Fujian, China, in 2016, where he is currently pursuing the master's degree. His main research interest includes the detection of arc faults.

XIAOQING GAO received the B.S. degree from the Henan University of Science and Technology, Henan, China, in 2017. He is currently pursuing the master's degree with Fuzhou University. His main research interest includes the detection of arc faults.